UNIVERSIDADE D COIMBRA

FACULDADE DE CIÊNCIAS E TECNOLOGIA

Influence of the orthotropic behaviour on defects prediction in cup drawing, reverse redrawing and expansions

Marta C. Oliveira[1] • Diogo M. Neto[1] • José L. Alves[2] • Luís F. Menezes[1]

[1] University of Coimbra, CEMMPRE, Department of Mechanical Engineering, Portugal

[2] University of Minho, CMEMS, Department of Mechanical Engineering, Portugal

VIRTUAL 2021 iddrg STUTTGART - GERMANY

22 June -2 July 2021
Online

Introduction

- The numerical simulation of cupping processes is fundamental for the can making industry.

- It allows the prediction of many different sheet metal defects and instabilities that significantly affect the efficient production of these parts.

- These defects include thinning from cup drawing, earing from plastic anisotropy, and damage and fracture from different combinations of strain paths, e.g. drawing and expansion.

Alcoa Shaping Technology

Dick R, Finite Element Modeling Applications to Canmaking, Invited lecture at University of Coimbra, 2018).

Benchmark 1 (Numisheet 2016): Benchmark 1 – Failure Prediction after Cup Drawing, Reverse Redrawing and Expansion

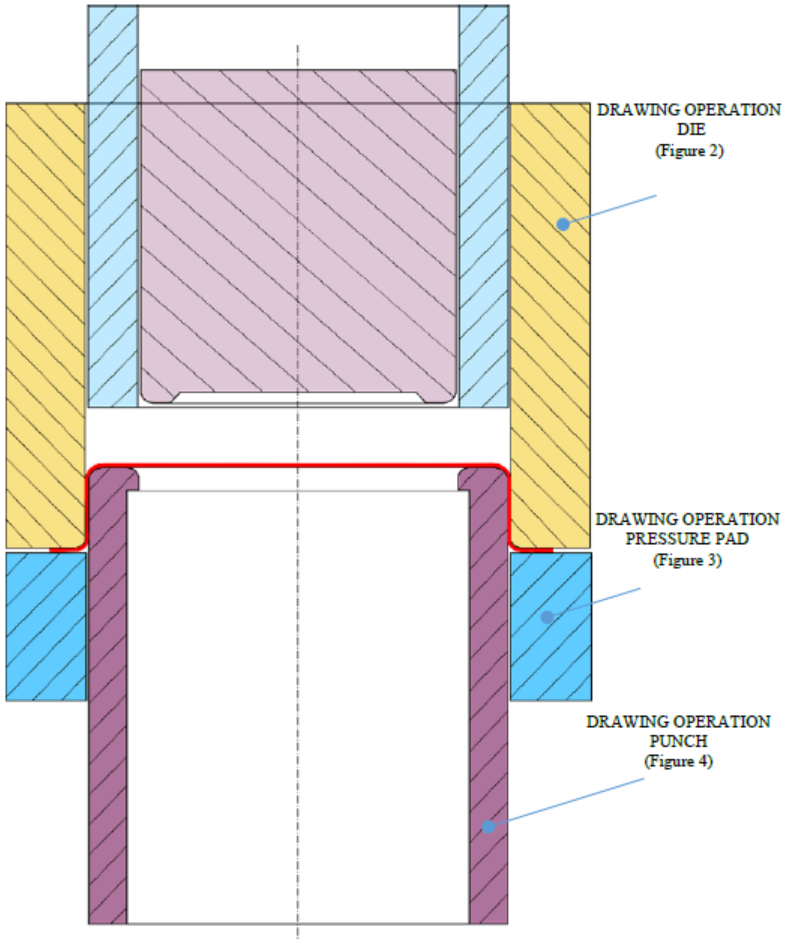

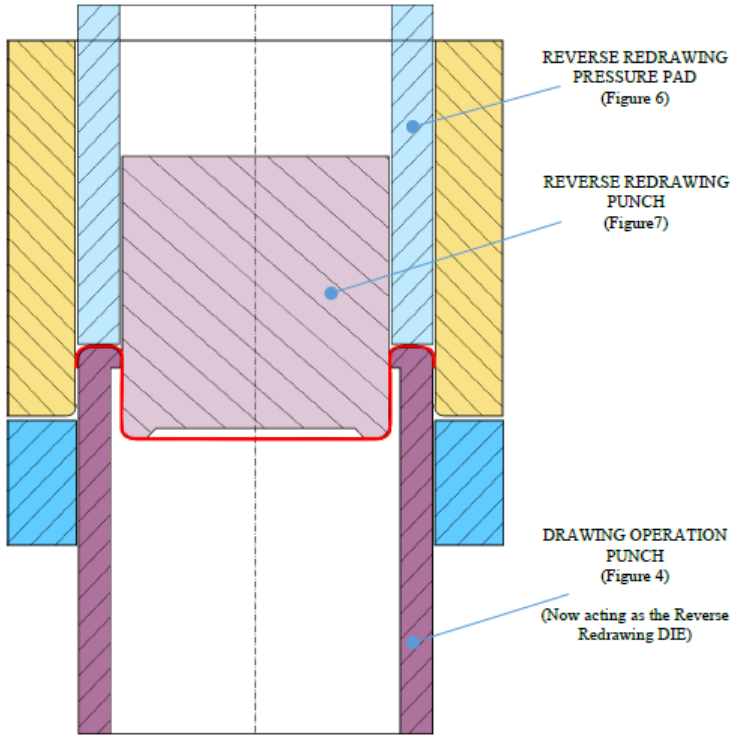

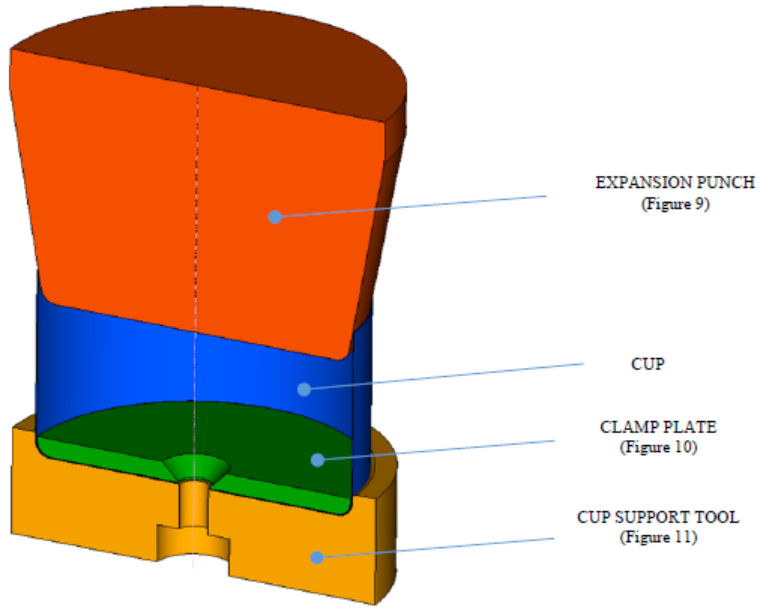

Setup for the: Drawing operation (left) Reverse Redrawing operation (center) and Practical setup for the die expansion operation

(Watson M, Dick R, Huang Y H, Lockley A, Cardoso R and Santos A 2016 Benchmark 1 - Failure Prediction after Cup Drawing, Reverse Redrawing and Expansion J. Phys. Conf. Ser. 734 022001).

Forming defects prediction

Benchmark 1 (Numisheet 2016): Benchmark 1 – Failure Prediction after Cup Drawing, Reverse Redrawing and Expansion

Steel cup **Aluminium cup**



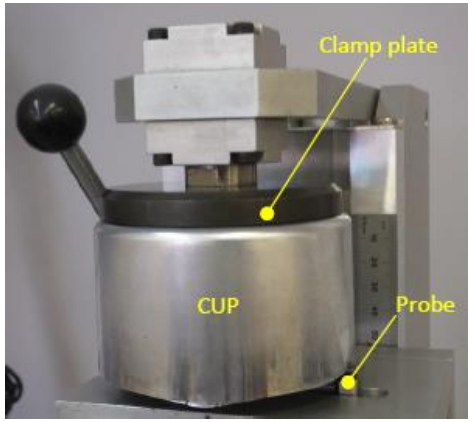

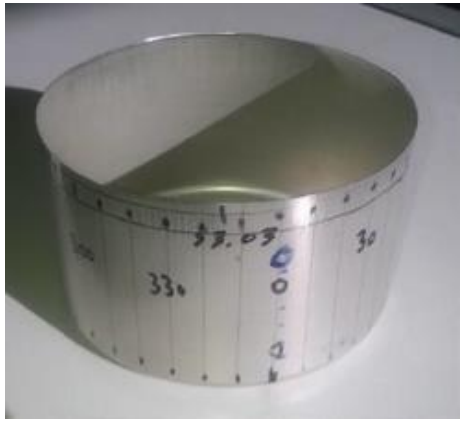


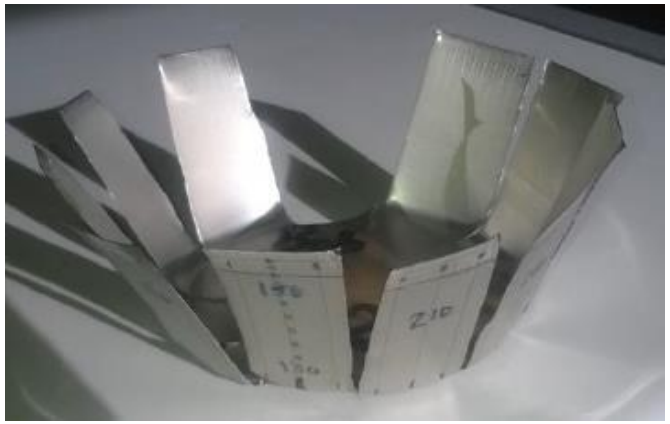


Cups after drawing and reverse redrawing (top-left); cups after expansion (bottom-left) and setups for earing and thickness measurements

(Watson M, Dick R, Huang Y H, Lockley A, Cardoso R and Santos A 2016 Benchmark 1 - Failure Prediction after Cup Drawing, Reverse Redrawing and Expansion J. Phys. Conf. Ser. 734 022001).

M.C. Oliveira (marta.oliveira@dem.uc.pt)

Benchmark 1 (Numisheet 2016): Benchmark 1 – Failure Prediction after Cup Drawing, Reverse Redrawing and Expansion

- The aims where the prediction:
  - of the earing, after the reverse redrawing operation;
  - of the thickness profile, after the reverse redrawing operation; and
  - of the failure point during the expansion operation.
- The blank sheet is circular with a diameter of 162.97 mm. Two materials with distinct orthotropic behaviour:
  - TH330 steel, with a thickness of 0.270 mm; and
  - AA5352 aluminium alloy, with a thickness of 0.279 mm.
- The drawing and reverse redrawing operations are performed considering a constant pressure-pad force, which is also equal for both materials:
  - Drawing operation: 21.1 kN; and
  - Redrawing: 16.6 kN.
- Recommend value for the constant friction coefficient of 0.03.

M.C. Oliveira (marta.oliveira@dem.uc.pt)

Failure Prediction after Cup Drawing, Reverse Redrawing and Expansion

Finite element model

- DD3IMP in-house finite element code (implicit time integration)
- 1/4 of the model (symmetry conditions)
- Forming tools are assumed rigid discretized by Nagata patches
- The Coulomb friction law is adopted, constant $\mu = 0.03$
- Blank discretized by linear hexahedral (8-nodes) finite elements (2 layers through the thickness)

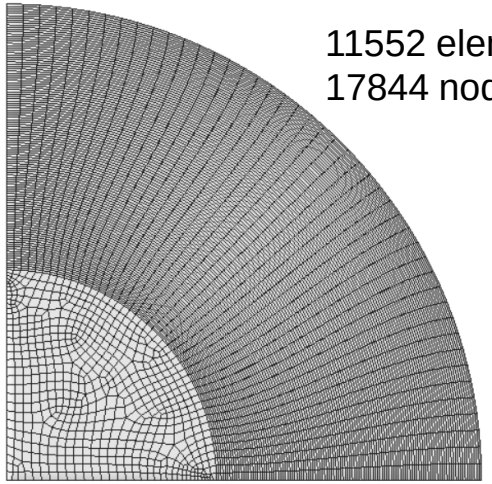

11552 elements
17844 nodes

Discretization of the blank with hexahedral finite elements.

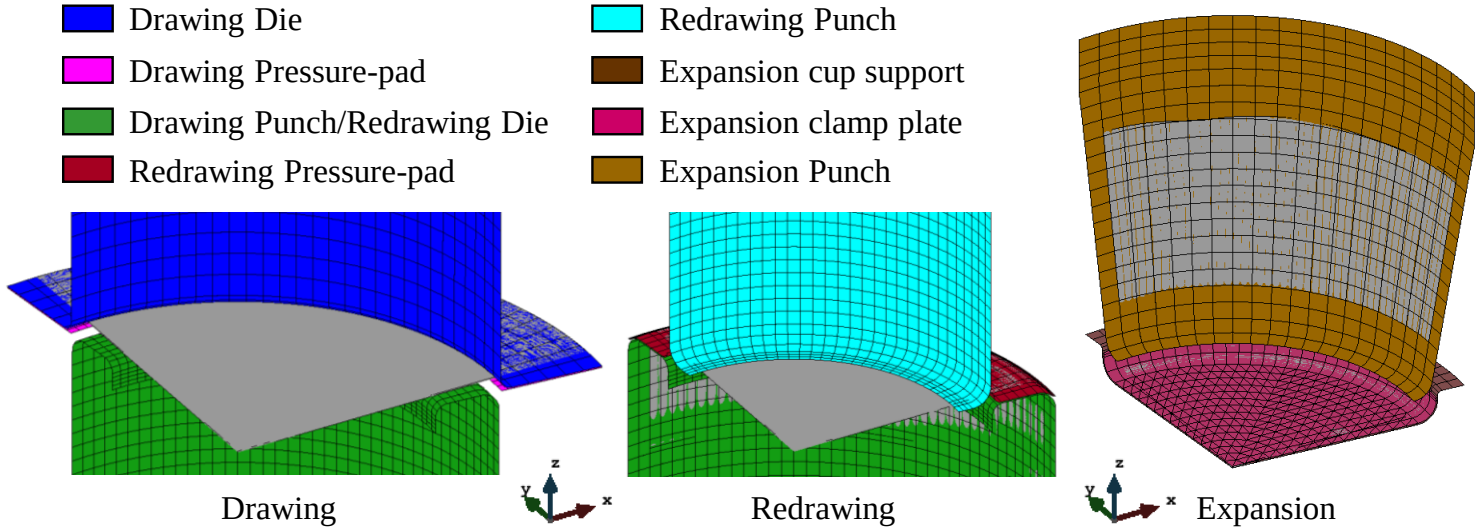

Numerical model: Nagata patches used to describe the surfaces of each tool.

Finite element model

- Isotropic elastic behaviour described with the Hooke's law.
- Isotropic hardening law determined by best fit for the stress-plastic strain curve, from the uniaxial test performed in the rolling direction (RD).

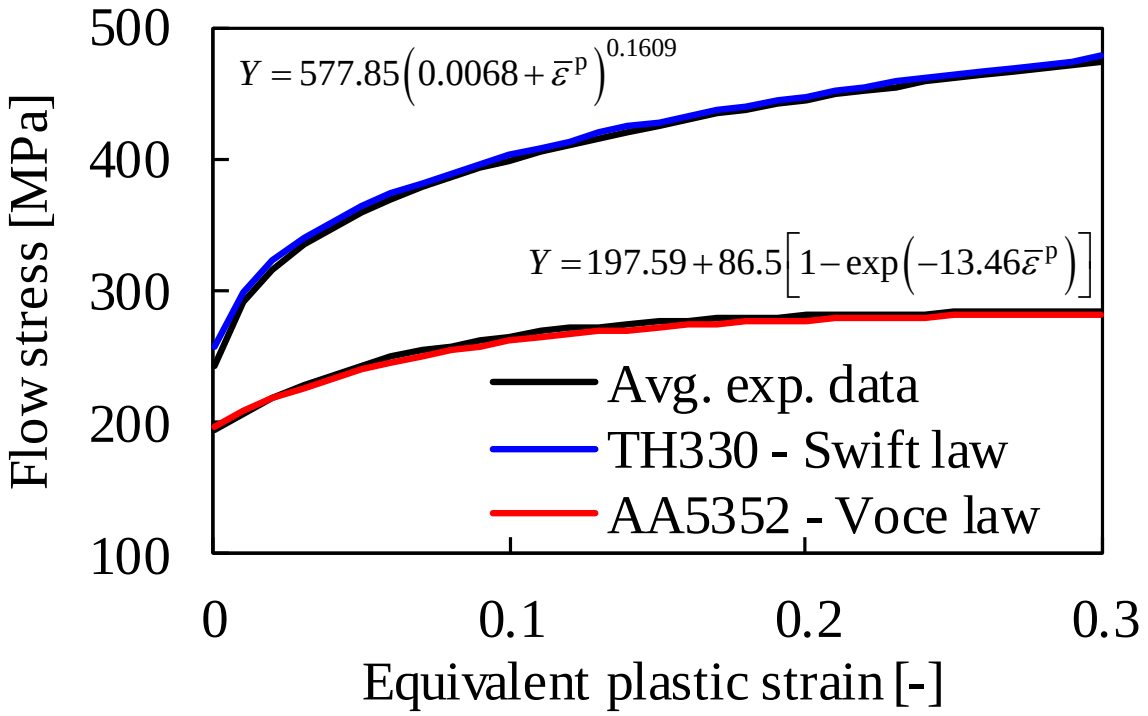

Stress–equivalent plastic strain curve and hardening law fitted from the uniaxial tensile test in RD.

Test	TH330 steel		AA5352 aluminium	
θ	r	σ_θ/Y_0	r	σ_θ/Y_0
0º	1.449	1.000	0.535	1.000
15º	1.373	0.998	0.465	0.979
30º	1.301	0.983	0.655	0.995
45º	1.266	0.986	1.105	0.982
60º	1.335	0.971	1.415	0.997
75º	1.443	0.967	1.595	0.996
90º	1.510	0.963	2.270	1.006
Biaxial	0.984	1.198	0.620	1.225

r-values and normalized yield stress values extracted from uniaxial tensile tests; biaxial stress extracted from bulge test and r_b extracted from disk compression test.

Cazacu and Barlat, 2001 (CB2001)

$$\left(J_2^0\right)^3 - c\left(J_3^0\right)^2 = 27\left(\frac{Y}{3}\right)^6$$

$$J_2^0 = \frac{a_1}{6}(\sigma_{11}-\sigma_{22})^2 + \frac{a_2}{6}(\sigma_{11}-\sigma_{33})^2 + \frac{a_3}{6}(\sigma_{11}-\sigma_{33})^2 + a_4\sigma_{12}^2 + a_5\sigma_{13}^2 + a_6\sigma_{23}^2$$

$$\begin{aligned} J_3^0 = {} & (1/27)(b_1+b_2)\sigma_{11}^3 + (1/27)(b_3+b_4)\sigma_{22}^3 \\ & + (1/27)[2(b_1+b_4)-b_2-b_3]\sigma_{33}^3 \\ & - (1/9)(b_1\sigma_{22}+b_2\sigma_{33})\sigma_{11}^2 - (1/9)(b_3\sigma_{33}+b_4\sigma_{11})\sigma_{22}^2 \\ & - (1/9)[(b_1-b_2+b_4)\sigma_{11} + (b_1-b_3+b_4)\sigma_{22}]\sigma_{33}^2 \\ & + (2/9)(b_1+b_4)\sigma_{11}\sigma_{22}\sigma_{33} \\ & - (\sigma_{13}^2/3)[2b_9\sigma_{22} - b_8\sigma_{33} - (2b_9-b_8)\sigma_{11}] \\ & - (\sigma_{12}^2/3)[2b_{10}\sigma_{33} - b_5\sigma_{22} - (2b_{10}-b_5)\sigma_{11}] \\ & - (\sigma_{23}^2/3)[(b_6-b_7)\sigma_{11} - b_6\sigma_{22} - b_7\sigma_{33}] + 2b_{11}\sigma_{12}\sigma_{23}\sigma_{13} \end{aligned}$$

Anisotropy parameters

a_1, a_2, a_3, a_4

$b_1, b_2, b_3, b_4, b_5, b_{11}$

Weighting coefficient

c

M.C. Oliveira (marta.oliveira@dem.uc.pt)

DD3MAT: objective function

$$F(\mathbf{A}) = w_{\sigma_\theta} \sum_\theta \left(\sigma_\theta \left(\mathbf{A}, \bar{\varepsilon}^{\mathrm{p}} \right) / \sigma_\theta \left(\bar{\varepsilon}^{\mathrm{p}} \right) - 1 \right)^2 + w_{r_\theta} \sum_\theta \left(r_\theta (\mathbf{A}) / r_\theta - 1 \right)^2$$
$$+ w_{\sigma_b} \left(\sigma_b \left(\mathbf{A}, \bar{\varepsilon}^{\mathrm{p}} \right) / \sigma_b \left(\bar{\varepsilon}^{\mathrm{p}} \right) - 1 \right)^2 + w_{r_b} \left(r_b \left(\mathbf{A}, \bar{\varepsilon}^{\mathrm{p}} \right) / r_b \left(\bar{\varepsilon}^{\mathrm{p}} \right) - 1 \right)^2$$

$\mathbf{A}$ – set of anisotropy parameters

σ_θ – yield stresses in uniaxial tension

r_θ – anisotropy coefficients in uniaxial tension

σ_b – yield stresses in biaxial tension

r_b – anisotropy coefficient in biaxial compression

w_i – weighting coefficients

- Minimized with a downhill simplex method.
- First approach: anisotropy parameters identified considering a similar weighting factor for all experimental data.
- For the AA5352 aluminium alloy, another identification performed, increasing the weight for the biaxial yield stress.

M.C. Oliveira (marta.oliveira@dem.uc.pt)

Identification of the anisotropy parameters

- **TH330 steel**: Based on the *r*-value and yield stress in-plane directionalities and on biaxial values.

c	a_1	a_2	a_3	a_4	b_1	b_2	b_3	b_4	b_5	b_{10}	**Others**
0.79	1.315	0.91	0.874	1.089	2.037	1.184	1.02	0.849	0.454	0.702	1.00000

- **AA5352 aluminium**: Based on the *r*-value and yield stress in-plane directionalities and on biaxial values.
  - With equal weighting values

c	a_1	a_2	a_3	a_4	b_1	b_2	b_3	b_4	b_5	b_{10}	**Others**
0.91	1.09	0.86	1.065	0.98	2.95	0.323	3.104	-1.804	-1.055	0.658	1.00000

  - With an higher weighting value for the biaxial stress

c	a_1	a_2	a_3	a_4	b_1	b_2	b_3	b_4	b_5	b_{10}	**Others**
1.532	1.293	0.527	0.992	0.868	2.944	-0.005	1.704	-1.882	-1.17	0.244	1.00000

M.C. Oliveira (marta.oliveira@dem.uc.pt)

Identification of the anisotropy parameters

- For the TH330 steel, the CB2001 recovers quite well the biaxial yield stress (experimental value of 310 MPa and analytical value of 306.8 MPa), the r_b (experimental value of 0.984 and analytical of 0.983), as well as the results from the uniaxial tensile tests.

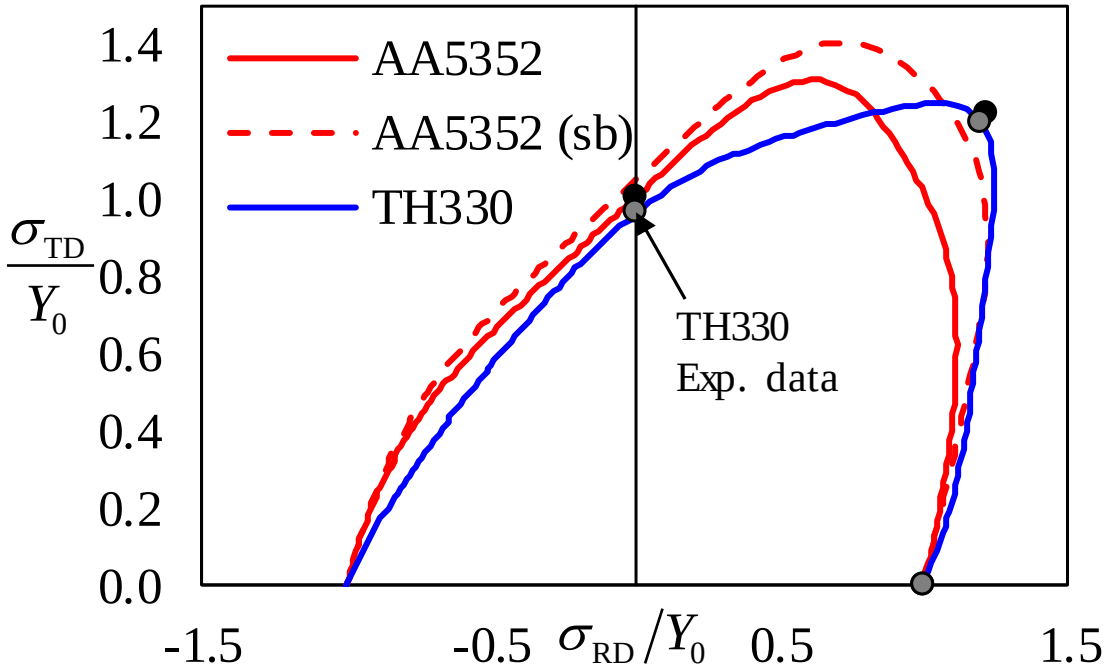

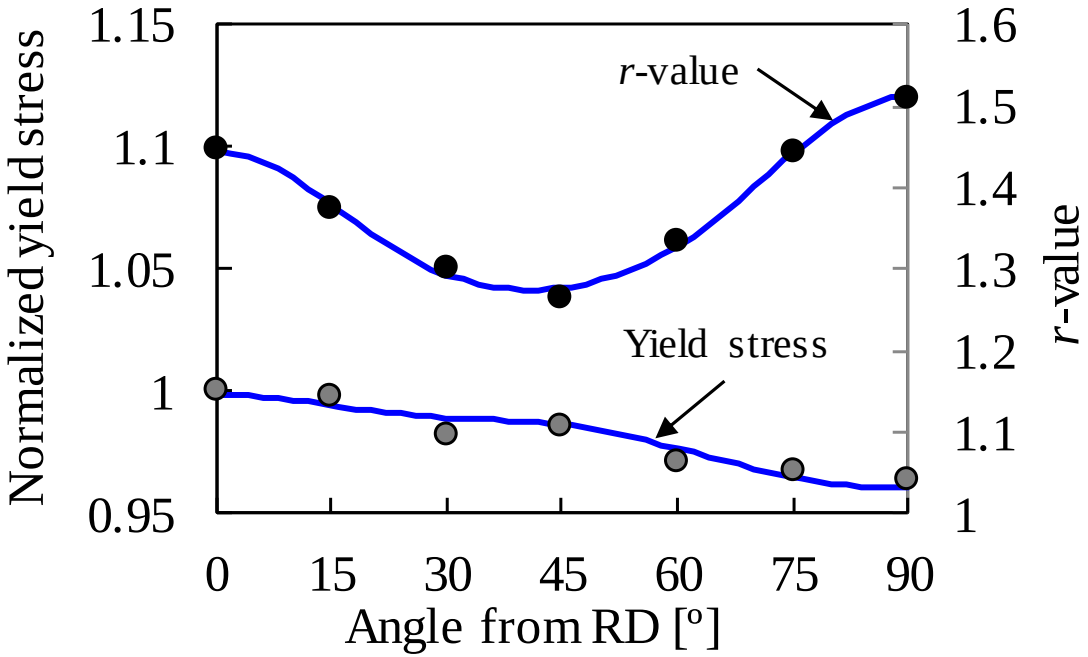

Projection of the yield surface in the biaxial plane (left) and experimental and predicted *r*-values and yield stresses for the TH330 steel.

M.C. Oliveira (marta.oliveira@dem.uc.pt)

Identification of the anisotropy parameters

- For the AA5352 aluminium alloy, the CB2001 only recovers quite well the biaxial yield stress (experimental value of 242.01 MPa and analytical value of 227.61 MPa), the r_b (experimental value of 0.620 and analytical of 0.643), when the weight for the biaixial value is increased.

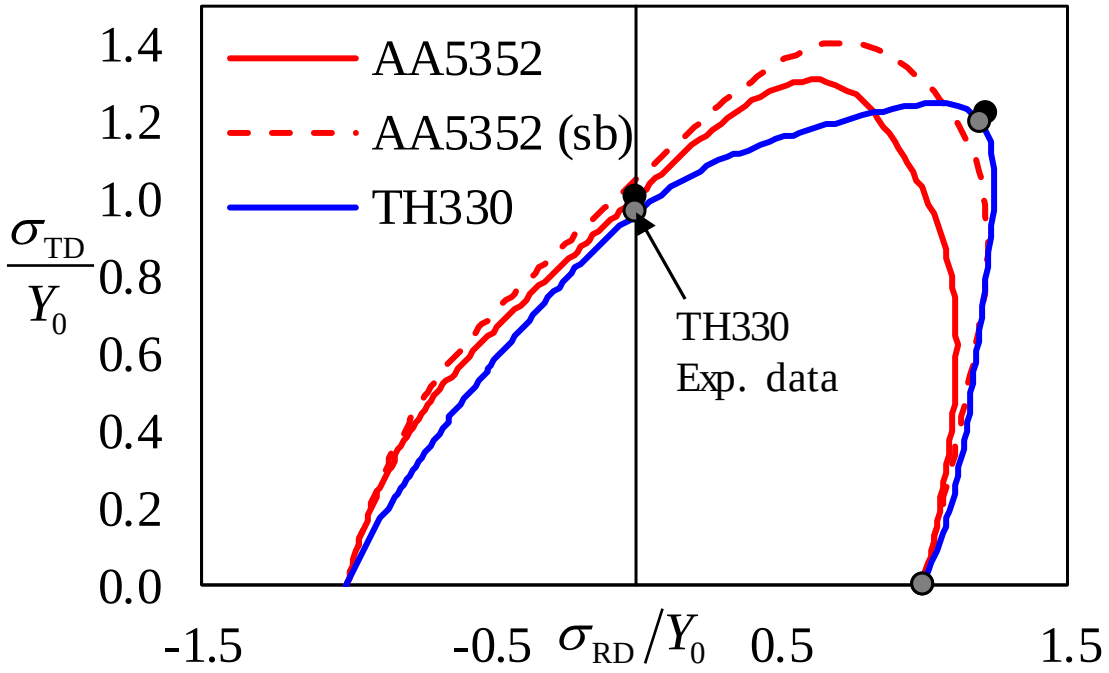

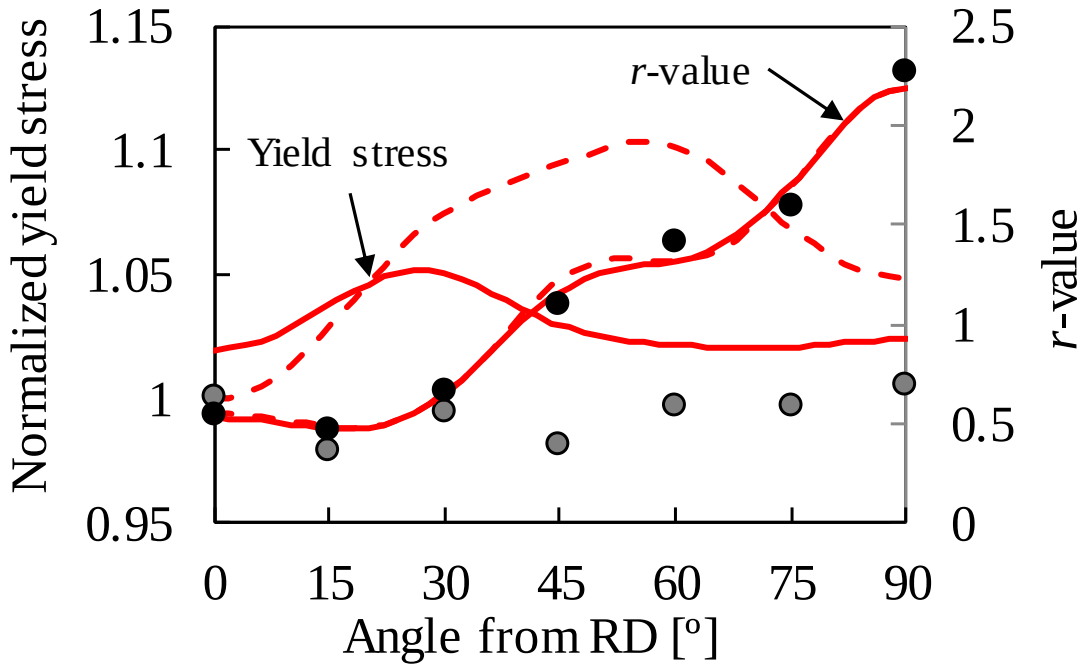

Projection of the yield surface in the biaxial plane (left) and experimental and predicted *r*-values and yield stresses for the AA5352 aluminium.

M.C. Oliveira (marta.oliveira@dem.uc.pt)

Failure Prediction after Cup Drawing, Reverse Redrawing and Expansion

Finite element model: AA5352 aluminium

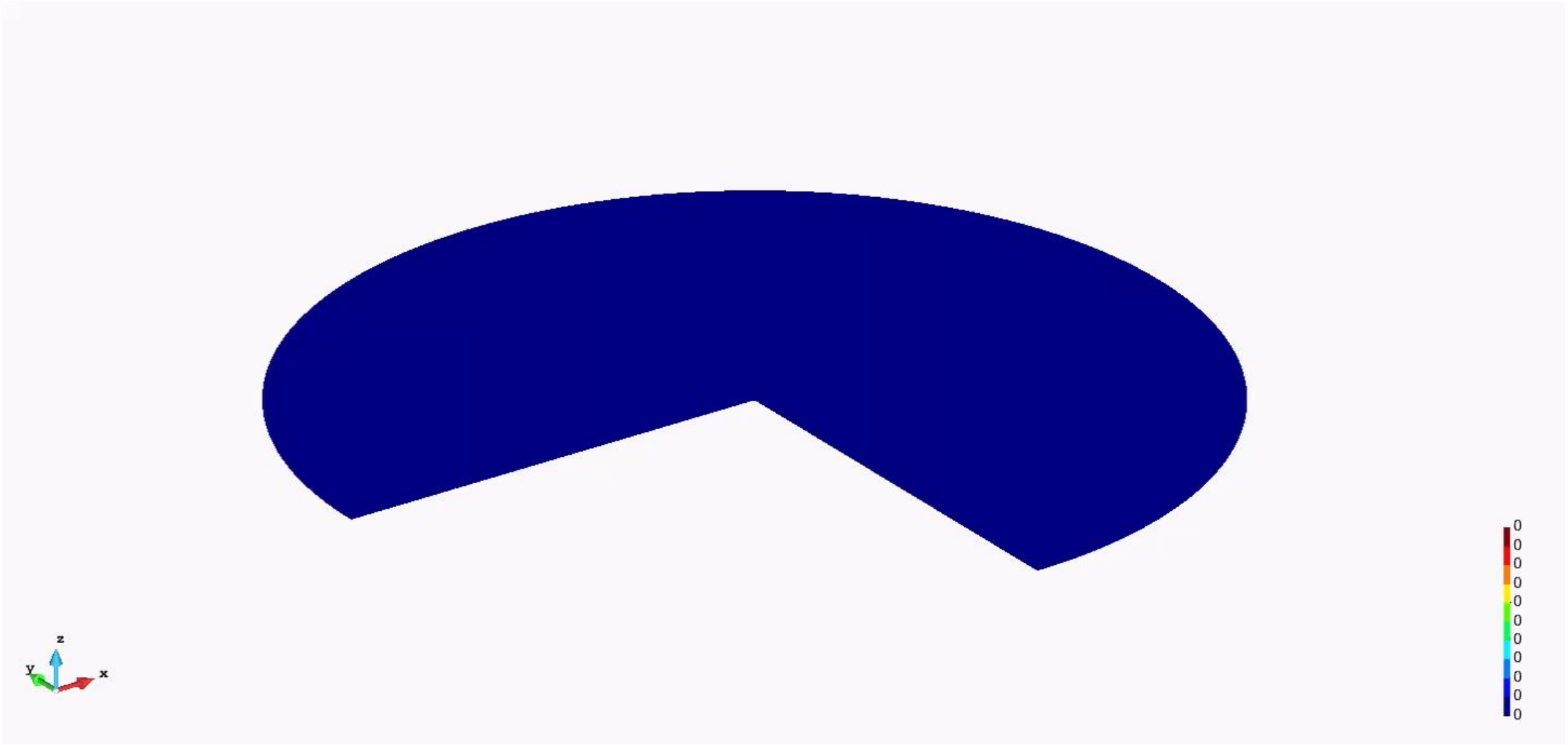

M.C. Oliveira (marta.oliveira@dem.uc.pt)

Failure Prediction after Cup Drawing, Reverse Redrawing and Expansion

Drawing force

- The “AA5352 (sb)” results in slightly higher values of force than for “AA5352”, which can be related with the globally higher yield stress in-plane directionalities.
- The expansion punch force presents a linear trend with its stroke, which is clearly underestimated, for both materials.

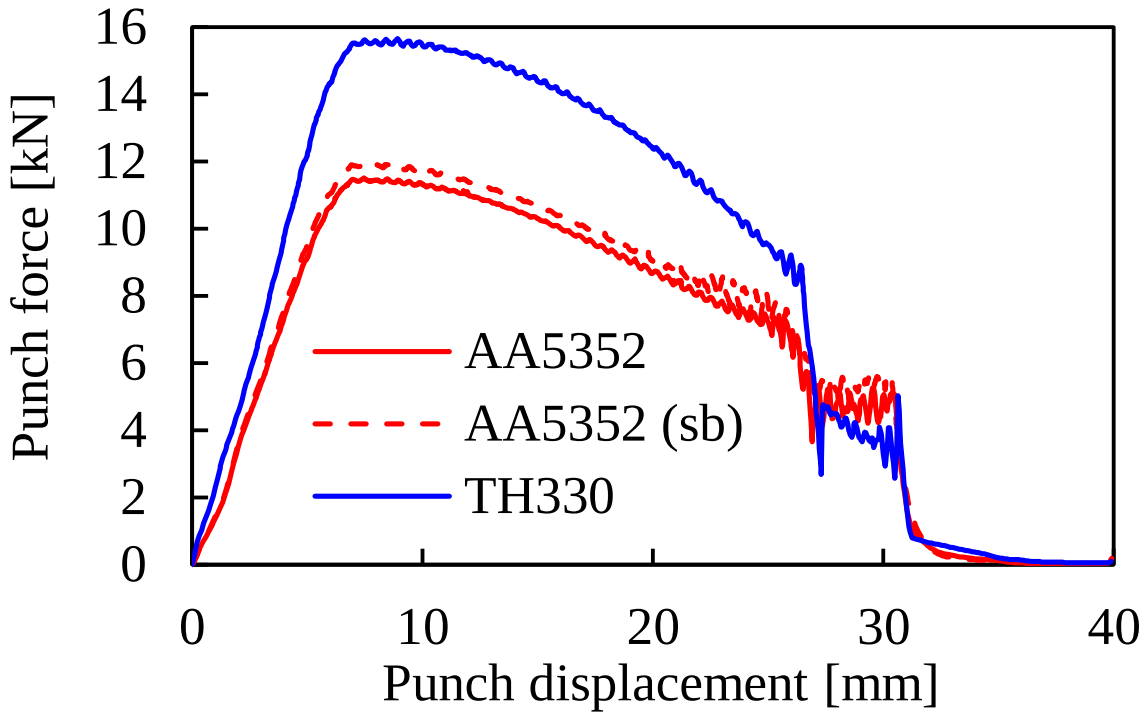

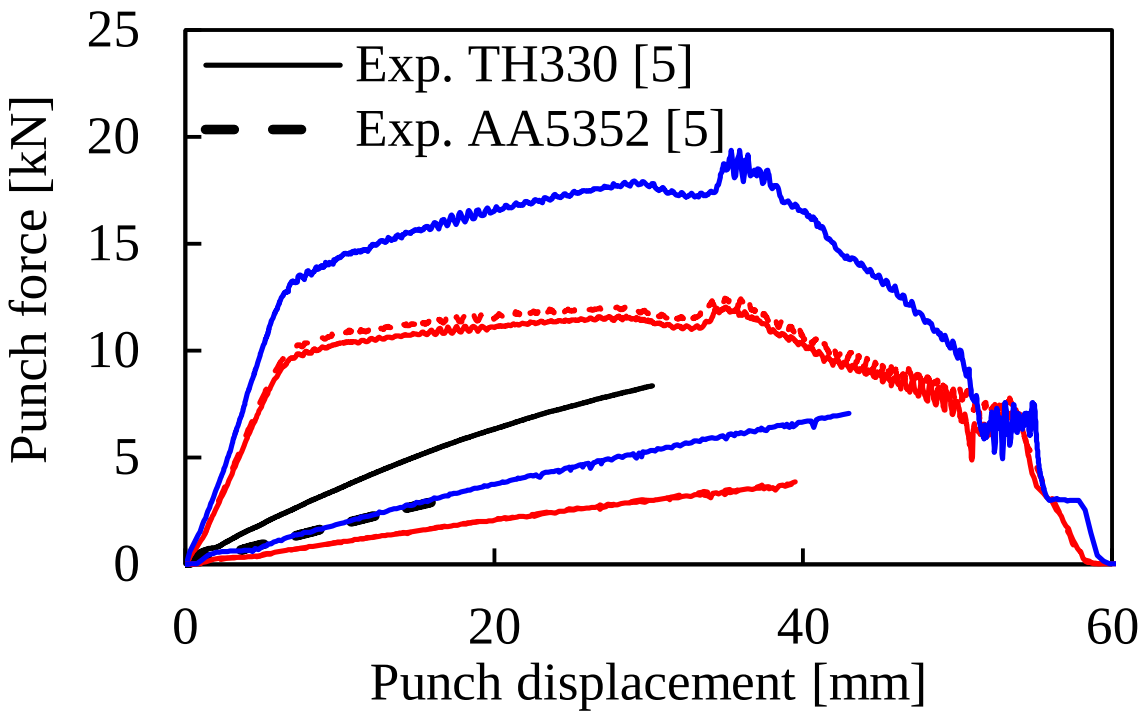

Comparison between experimental measurement and numerical prediction of the punch force evolution with the displacement in the drawing (left) and reverse redrawing and expansion (right).

Failure Prediction after Cup Drawing, Reverse Redrawing and Expansion

Earing profile

- The TH330 steel presents an almost constant height, with 4 ears more visible after redarwing.
- The AA5352 aluminium alloy presents a total of 8 ears, which have a higher amplitude for the “AA5352 (sb)”. However, the trend for the height is not well captured, because at TD it is clearly overestimated, by both sets of anisotropy parameters.

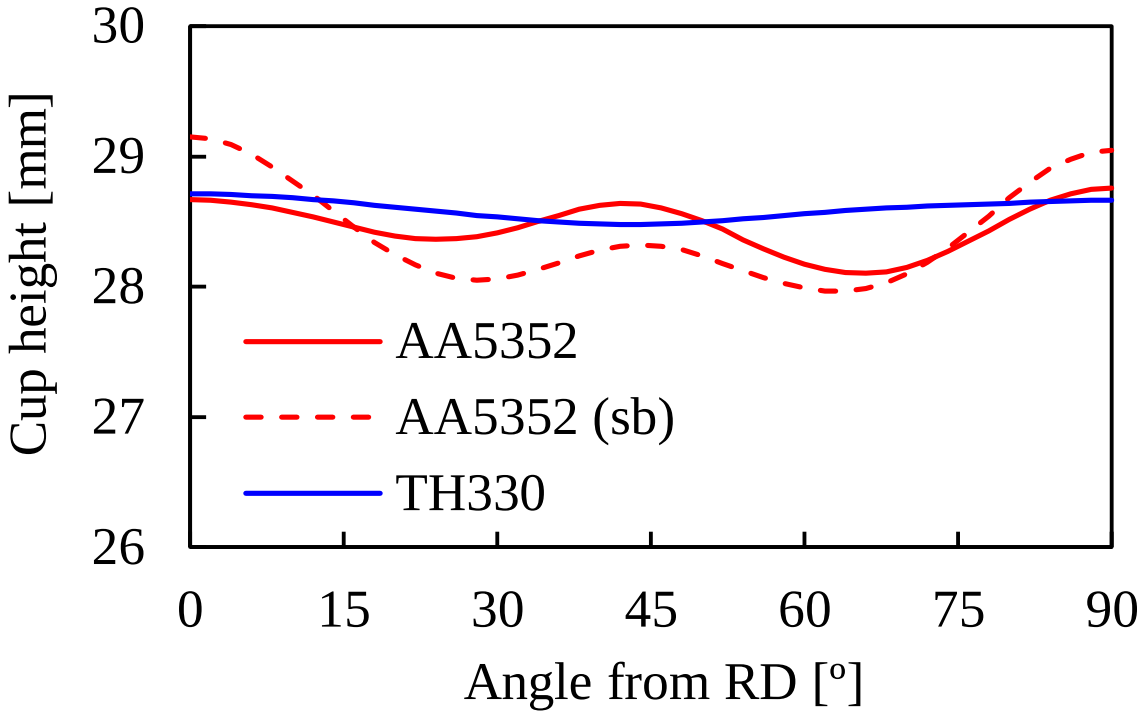

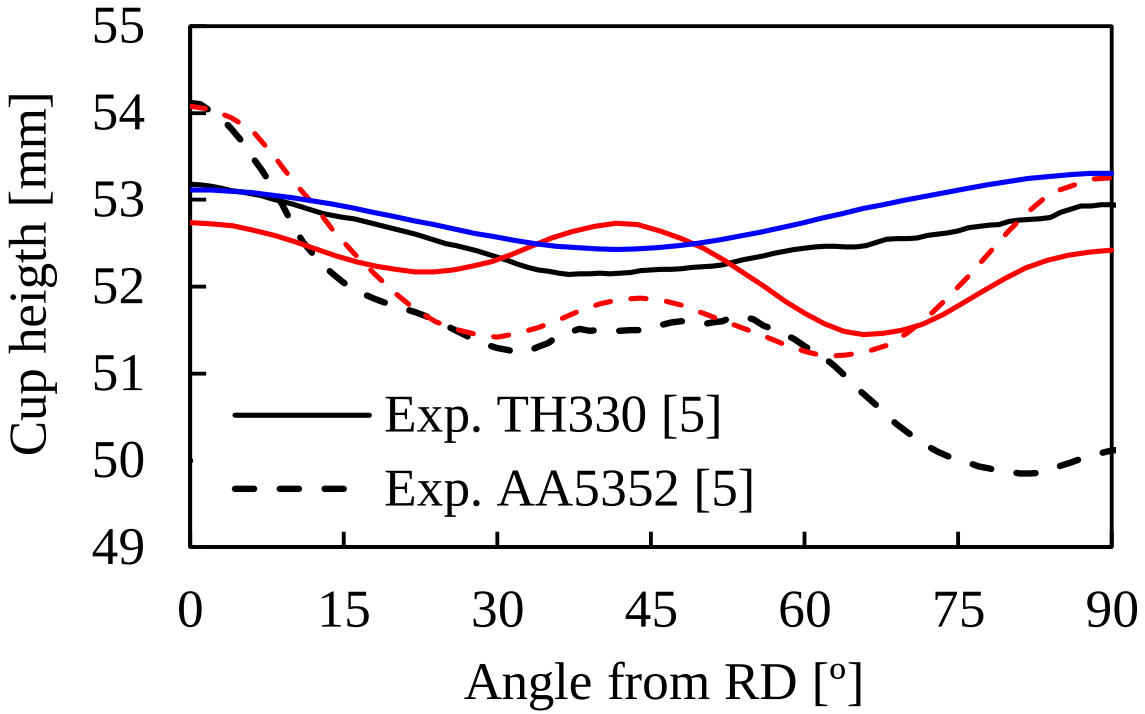

Comparison between experimental and predicted up height, in function of the angle from RD, at the end of the drawing (left) and reverse redrawing (right).

M.C. Oliveira (marta.oliveira@dem.uc.pt)

Failure Prediction after Cup Drawing, Reverse Redrawing and Expansion

Earing profile

- For the AA5352 aluminium alloy, at the end of the redrawing stage there are some areas with strong thinning at the top of the cup. For “AA5352” this occurs at the RD and close to 45º with RD, while for “AA5352 (sb)” it disappears for 45º but appears at TD, and becomes more relevant at the RD.

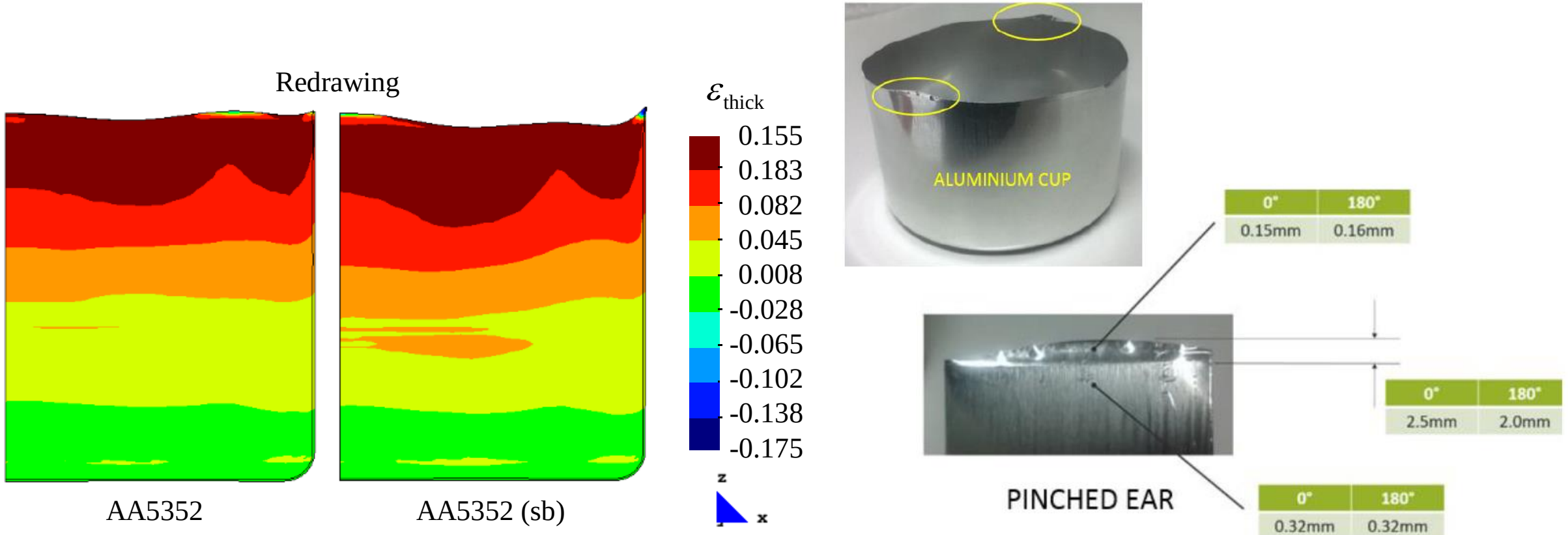

Distribution of the thickness strain at the end of the reverse redrawing, for the AA5352 aluminium alloy (left) and experimental analysis of the location of the pinched ears (right).

M.C. Oliveira (marta.oliveira@dem.uc.pt)

Failure Prediction after Cup Drawing, Reverse Redrawing and Expansion

Thickness distribution

- For the TH330 steel, the numerical values are always bellow the experimental range.
- For the AA5352 aluminium alloy, the numerical values are close to the minimum value of the experimental range. Moreover, the experimental results present an increasing trend between RD and TD, while the numerical are almost constant value. Note that there was some ironing of the vertical wall during the redrawing stage.

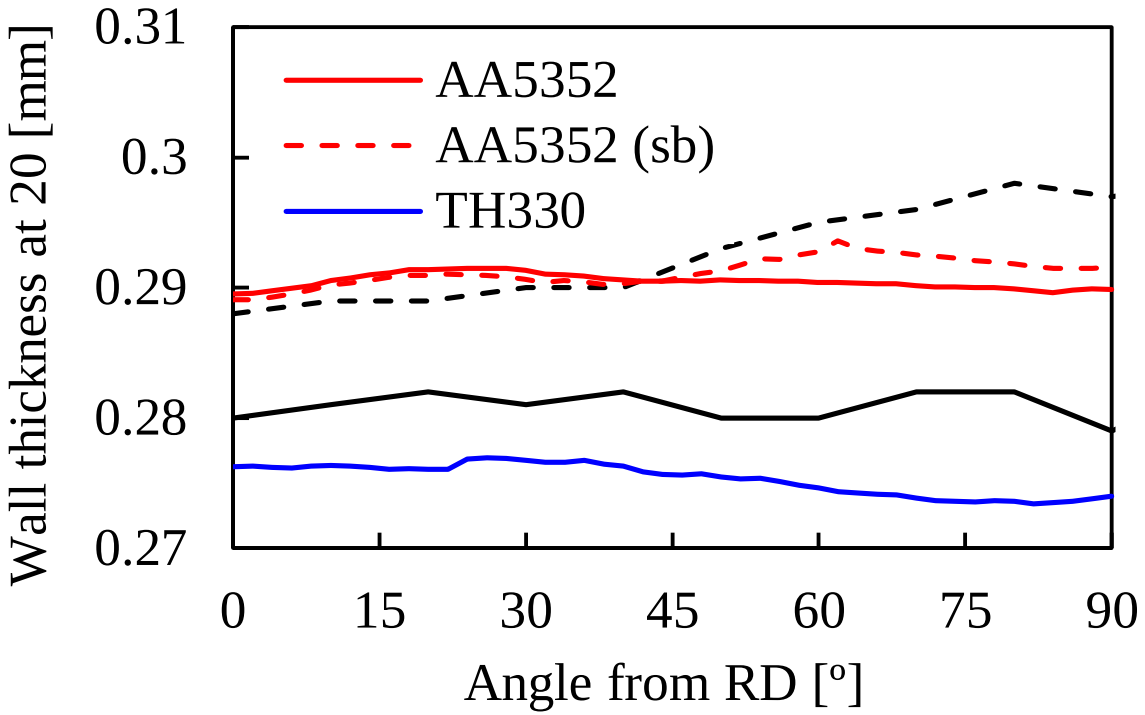

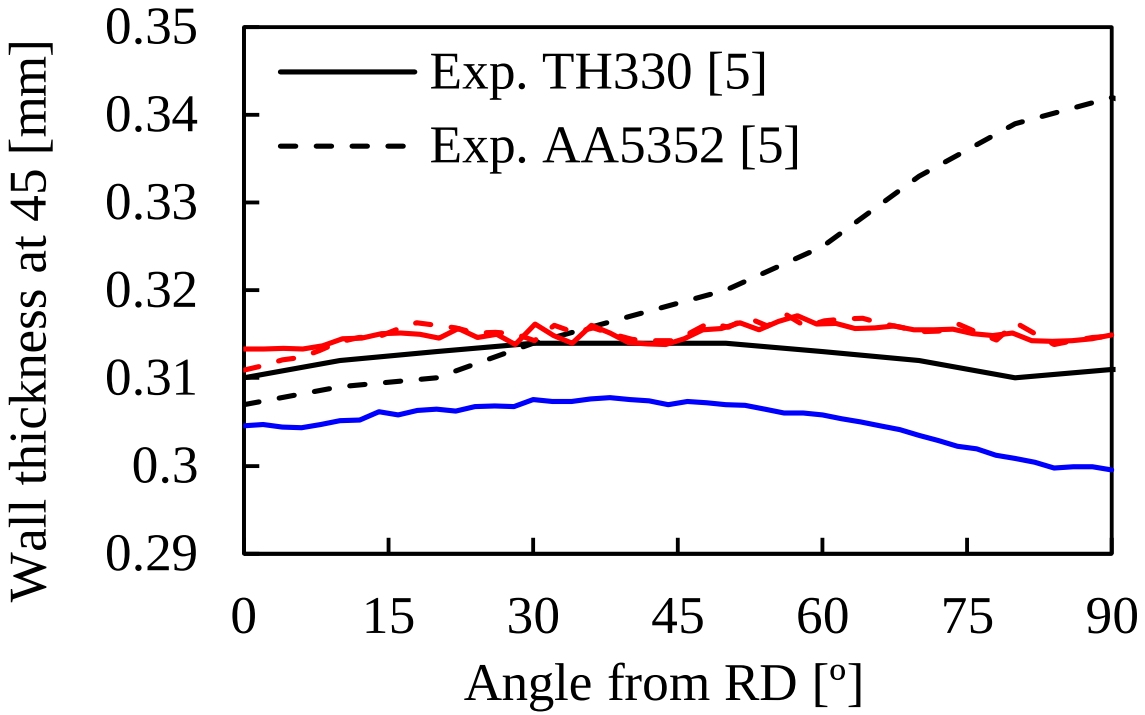

Comparison between experimental and predicted results for the wall thickness in function of the angle from RD, at the end of the reverse redrawing operation, at a distance from the cup base of 20 mm (left) and 45 mm (right).

M.C. Oliveira (marta.oliveira@dem.uc.pt)

Failure Prediction after Cup Drawing, Reverse Redrawing and Expansion

Fracture during expansion

- For the TH330 steel, there is no strain localization in the part.
- For the AA5352 aluminium alloy, the strain localization is predicted by both sets of anisotropy parameters, for similar displacements of the expansion punch and at identical orientations with RD. Both numerical results overestimate the punch displacement and the location is not that close to TD.

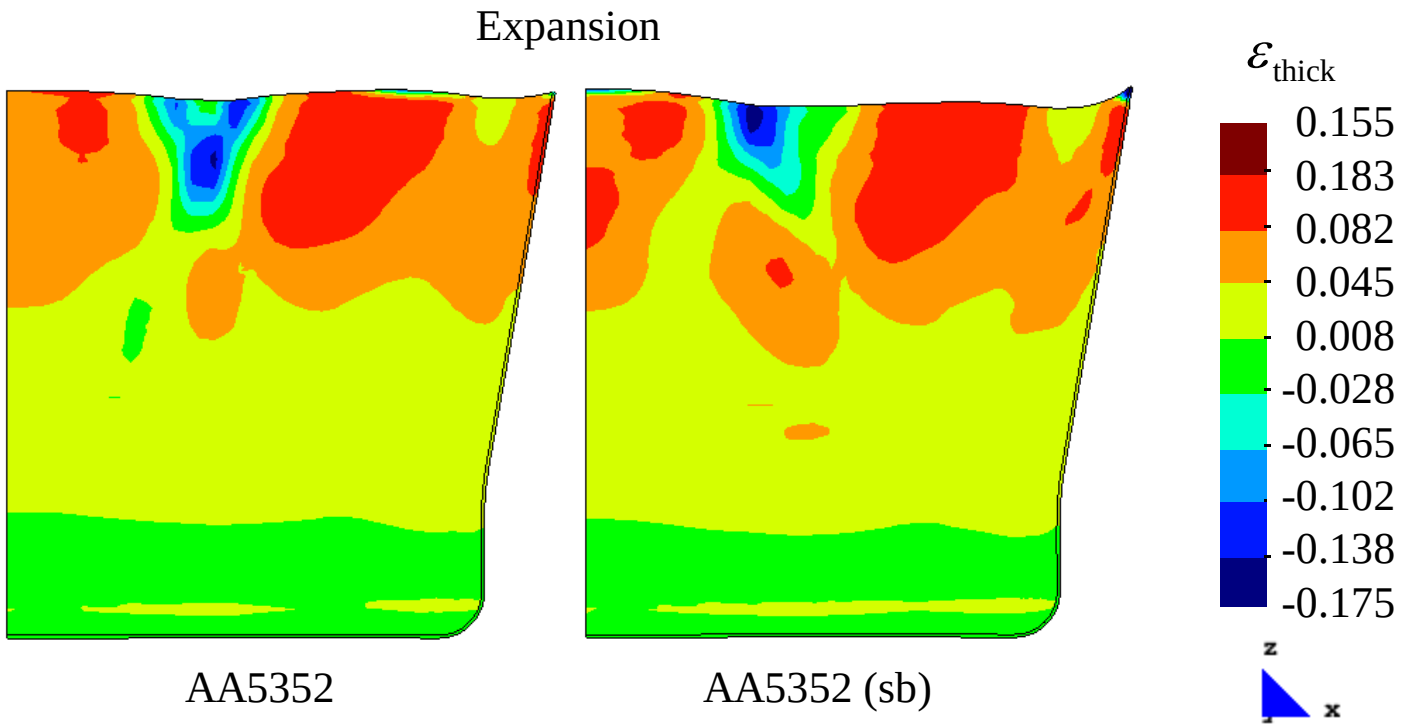

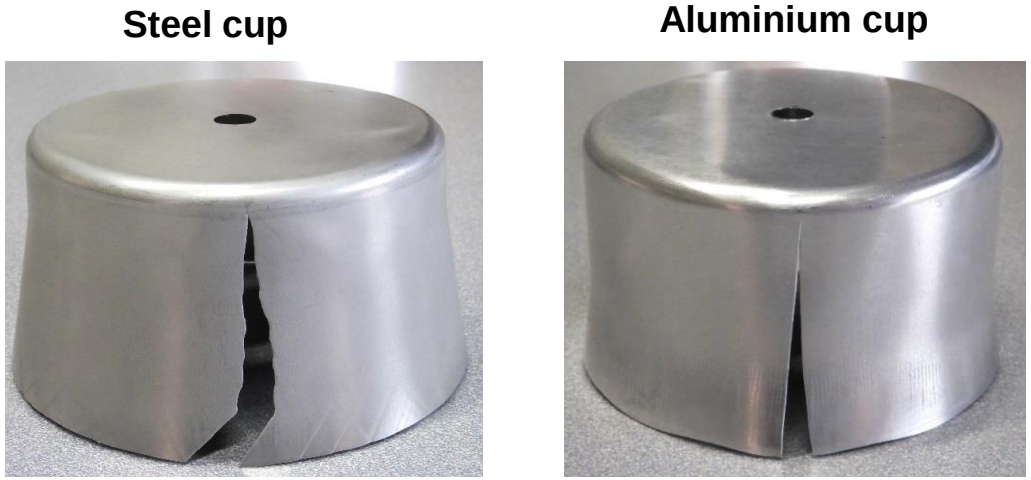

Distribution of the thickness strain at the end of the expansion phase, for the same punch displacement, for the AA5352 aluminium alloy (left) and cups after expansion (right).

M.C. Oliveira (marta.oliveira@dem.uc.pt)

Failure Prediction after Cup Drawing, Reverse Redrawing and Expansion

Strain paths

- Globally, the points follow a more dissimilar trend for the AA5352, highlighting the fact that this material presents a more anisotropic behaviour than the TH330 steel.
- For the AA5352 higher major strains are attained, particularly at the end of the reverse redrawing operation, which can be related with the ironing stage.

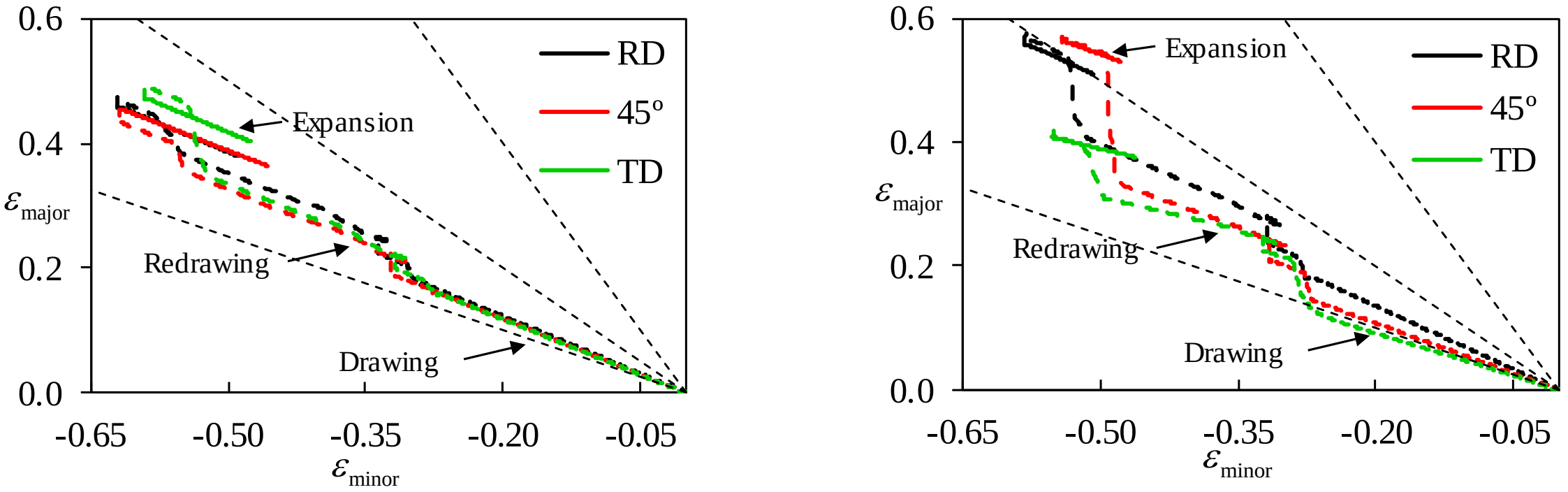

Evolution of the principal in-plane strains at the leading edge of the cup at RD, 45º with RD and TD for the TH330 steel (left) and the AA5352 aluminium alloy.

M.C. Oliveira (marta.oliveira@dem.uc.pt)

Conclusions

- Globally, the cup height at the end of the reverse redrawing operations is well predicted.

- Nonetheless, the thickness distribution along the cup circumferential direction is underestimated, for both materials.

- For the AA5352 aluminium alloy this can be related with the occurrence of ironing of the wall in the numerical simulation, since the gap between the die and the punch of the redrawing stage does not allow to accommodate the thickening that occurs in the flange. Thus, the discrepancy can be associated with different process conditions.

- However, the result indicate that the plastic flow is not accurately described by the normal to the yield surface. The analysis of the strain history highlights the importance of the stress states located between uniaxial compression and pure shear. Unfortunately, this region of the yield surface is not covered by the set of experimental mechanical tests performed to characterize the mechanical behaviour of the material.

M.C. Oliveira (marta.oliveira@dem.uc.pt)

Acknowledgements

The authors would like to acknowledge the funding from of the **Foundation for Science and Technology** (FCT) under projects with reference PTDC/EME-EME/30592/2017 and PTDC/EME-EME/31243/2017 and by **European Regional Development Fund** (ERDF) through the Portugal 2020 program and the Centro 2020 Regional Operational Programme (CENTRO-01-0145-FEDER-031657) under project MATIS (CENTRO-01-0145-FEDER-000014) and UIDB/EMS/00285/2020.

The authors would also like to acknowledge Doctor **Robert Dick** for sharing the experimental data and for the helpful discussions.

Projetos Cofinanciados pela UE:

FCT Fundação para a Ciência e a Tecnologia

CENTRO 2020

PORTUGAL 2020

UNIÃO EUROPEIA
Fundo Europeu de Desenvolvimento Regional